Geotech Geol Eng (2018) 36:551–566
https://doi.org/10.1007/s10706-017-0346-1

ORIGINAL PAPER

R&D and Application of Curved D-Shape Concrete-Filled Steel Tube Support in Roadway Support

Jin-peng Zhang · Li-min Liu

Received: 28 February 2017 / Accepted: 18 August 2017 / Published online: 8 September 2017

Abstract The concrete-filled steel tube support (CFSTS) has been proposed as a new passive support form for controlling the stability of surrounding rock in underground structures, especially for the case of high ground stress. In order to improve the application of the CFSTS in the high stress soft rock roadway, this paper made a comparison between the commonly used U36 steel support and the CFSTS, and the advantages of the CFSTS were determined by theoretical calculation; By using the numerical simulation to optimize the ordinary CFSTS, the D-shape concrete-filled steel tube support (D-CFSTS) was designed, then the compression analysis was carried out; Based on the engineering background of the Pingdingshan ten mines, the D-CFSTS was applied to the support of the soft rock roadway. The results show: The supporting force of the CFSTS is far greater than that of the U-steel support. Under the same load, the deformation of the D-CFSTS is smaller than that of the circular CFSTS, especially D-CFSTS is more suitable for the deep roadway where the horizontal stress is greater than the vertical stress. In the Pingdingshan ten mines, the U-steel support was damaged prematurely, but the D-CFSTS had good effect and could maintain long-term stability.

Keywords D-shape steel tube · CFSTS · U-steel support · D-CFSTS · Roadway support

1 Introductions

Coal has been dominant in China's energy economy. However, the shallow coal resources have been increasingly scarce after years of mining, coal mining has gradually turned to deep. The geological conditions in deep mine are so complex that the support of soft rock roadway with high stress is very difficult (Yang et al. 2017; Meng et al. 2012). Traditional bolt and U-steel support can not meet the support requirements of high stress soft rock roadway. Soft rock roadway support has always been an important and complicated technical problem in the underground engineering in the world. So whether it can solve the problem of soft rock roadway support is the key to the development of mine exploitation in depth and safety.

The biggest disadvantage of U-steel support is that the connection point can not reach its own strength requirement and the utilization ratio of steel is low. Because the horizontal stress is greater than the vertical stress in the high stress roadway of deep well, the column leg of U-steel support is damaged firstly, which leads to lower overall support force. Concrete-

J. Zhang · L. Liu (✉)
College of Mining and Safety Engineering, Shandong University of Science and Technology, Qingdao 266590, Shandong, China
e-mail: zhljinpeng@163.com

L. Liu
e-mail: 2280840483@qq.com

filled steel tube (CFST) has the advantages of high bearing capacity, corrosion resistance and easy construction, which has been widely used in civil engineering. Some scholars have carried out extensive research on the performance of CFST structures (Guo et al. 2012; Nie et al. 2014; Gu et al. 2014). When the concrete is poured in the steel tube and reaches a certain strength, the local stability of thin wall steel tube is guaranteed by the concrete. Conversely, the steel tube restrains the radial deformation of the concrete and makes it in the triaxial stress state. So, the time of the longitudinal cracking of concrete is delayed and the bearing capacity of CFST members is improved (Dong et al. 2017). As a composite material, CFST has unique characteristics: elastic work and plastic failure, high bearing capacity and large extreme compression deformation (Aghdamy et al. 2015; Thayalan et al. 2009; Han et al. 2009).

According to the application of CFST in civil engineering area, it is extended to mine roadway support and the CFSTS structure is developed. CFSTS is a new type of high strength support of R&D success in recent years. In the support of soft rock roadway, CFSTS can provide strong supporting force, control the deformation of the roadway and maintain the stability of the roadway. Gao et al. (2010), Wang (2009) and Gao et al. (2009) has put forward the concrete-filled steel tube support for controlling the stability of surrounding rock in underground structures and has carried on experiments and applications. Xu et al. (2014) presented a numerical study on the mechanical performance of CFT support.

In order to improve the application of CFSTS in the high stress soft rock roadway, this paper made a systematic study on the CFSTS based on the existing CFSTS. Firstly, the bearing capacity of U-steel support and CFSTS was calculated and analyzed. Then, the CFSTS was optimized and the D-CFSTS was put forward by the numerical simulation. Finally, combined with the high stress soft rock roadway of Pingdingshan ten mines, the engineering application research was carried out.

2 Theoretical Calculation of Supporting Force

In order to compare and analyze whether the CFSTS is superior, the mechanical calculation models of U-steel support and CFSTS were established and the ultimate bearing capacity of U-steel support and CFSTS was calculated, respectively. Further, it was analyzed whether the U-steel support and the CFSTS meet the requirements of the deep mine.

2.1 Supporting Force of U-Steel Support

Now, U-steel support is used widely in coal mine. U36 was chosen as an example to calculate the U36 supporting capacity in this paper. To simplify the calculation, the semi-circular arch U-steel support was chosen as the research object. It is assumed that the arch part of U-steel support is subjected to uniform load of q and the lateral pressure coefficient of mine is k. So, the U-steel support leg is subjected to the lateral pressure of kq. In addition, the two legs are subjected to a vertical upward support force of N, respectively. The arch radius and the leg height of U-steel support are r and l. The main damage position of U-steel support in deep well is in the leg by bending moment, so the ultimate bearing capacity of U-steel support is determined by the leg. When the redundant constraint is removed, the U-steel support becomes the statically determinate structure. The hinged immovable support of U-steel support is changed into a hinged movable support. To maintain the stability of U-steel support, the horizontal thrust of F_T is applied to the structure (Zhou 2010). Figure 1 is the model of U-steel support. When only horizontal thrust is applied to the structure, the horizontal displacement δ_1 of the hinge support is:

$$\delta_1 = \frac{1}{EI}\left(\frac{2}{3}l^3 + \pi r l^2 + 4r^2 l + \frac{\pi}{2}r^3\right) \tag{1}$$

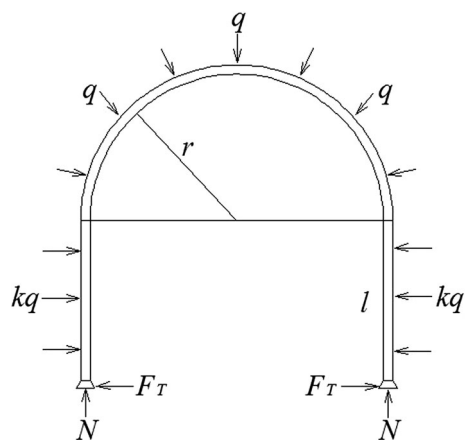

Fig. 1 Model of U-steel support

where, E represents elastic modulus of material; I represents material moment of inertia; r represents arch radius, 190 cm; l represents arch height, 160 cm.

The load q is acting alone on the basic structure, and the horizontal displacement of the bearing is:

$$\Delta_x = -\frac{kq}{EI}\left(\frac{1}{4}l^4 + \frac{1}{2}\pi rl^3 + 3r^2l^2 + \frac{1}{2}\pi r^3 l\right) \quad (2)$$

where, load at the top arch is q; The lateral load of the column leg is kq;This article studies the deep mine roadway, requires $k \geq 1$.

Horizontal thrust:

$$F_T = -\frac{\Delta 1p}{\delta 11} = \frac{3l^4 + 6\pi rl^3 + 36r^2l^2 + 6\pi r^3 l}{8l^3 + 12\pi rl^2 + 48r^2 l + 6\pi r^3} kq \quad (3)$$

Substituting the data of l, r, $F_T = 113.37kq$.

The maximum value $M_{\max}$ of the bending moment M of the support on the column leg is:

$$M_{\max} = \frac{1}{2} \cdot \frac{F_T^2}{kq} \quad (4)$$

Substituting the data of F_T, $M_{\max} = 6426.39kq$.

The maximum axial force $F_{N\max}$ of the column leg is:

$$F_{N\max} = -rq \quad (5)$$

Let the above:

$$M_{\max} = W_x(\sigma_s - F_{N\max}/A) \quad (6)$$

where, W_x represents section modulus of the maximum bending moment, the section modulus of U36 is 137 cm^3; σ_s represents Material yield limit, the type of steel is 16Mn, σ_s is 3500 KN/cm^2; A represents sectional area, the sectional area of U36 is 45.7 cm^2.

Substituting the data, $q = \frac{4795}{5.7+64.26k}$

The support force of the U-steel support is calculated:

$$F_b = \sum_{i=1}^{n} q_i l_i = (\pi r + 2l)q \quad (7)$$

When $k = 1$, $F_b = 628.24$ KN; when $k = 1.2$, $F_b = 530.71$ KN; when $k = 1.5$, $F_b = 430.53$ KN; when $k = 2$, $F_b = 327.41$ KN.

From the calculation and analysis, we can know that with the increase of the ratio of the lateral load on column legs and the vertical load on top arch, the supporting force of the support is gradually reduced. The typical characteristics of deep roadway are that horizontal stress is greater than vertical stress. Even the ratio of the horizontal stress and the vertical stress in some deep mine roadway are more than 1.5, so the U-steel support is not suitable for deep roadway, especially for the high level stress roadway.

2.2 Supporting Force of CFSTS

It is commonly agreed that there is a simple linear relationship between the ultimate bearing capacity of CFSTS and the axial bearing capacity of CFST short column. The axial compressive capacity of CFST short columns was calculated by establishing the mechanical model of CFST short columns. Futher, the ultimate bearing capacity of CFSTS was calculated.

1. Bearing capacity of short columns

It is assumed that the outer diameter of steel tube is D, the wall thickness of steel tube is δ and the axial compression of CFST short column, concrete column and steel tube are P, P_C, P_S. The mechanical model of CFST short column is established, as shown in Fig. 2. The cross section of CFST short columns is shown in Fig. 3.

The axial compression of CFST short column is the sum of the axial compression of concrete column and the axial compression of steel tube. That is:

$$P = P_S + P_C \quad (8)$$

The cross section area of steel tube:

$$A_s = \frac{\pi(D-\delta)^2}{4} \quad (9)$$

The cross section area of core concrete:

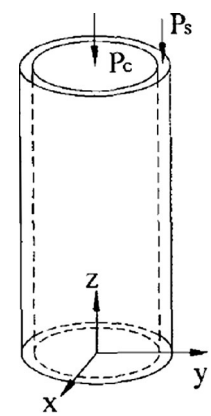

Fig. 2 The mechanical model of CFST short column

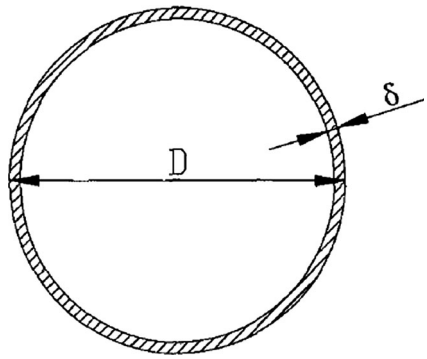

Fig. 3 The cross section of CFST short columns

$$A_c = \frac{\pi\delta(2D-\delta)}{4} \tag{10}$$

The ultimate axial compressive strength of CFST short column is obtained by the analysis and derivation.

$$P_{\max} = A_c f_c(1+\sqrt{\theta}+1.1\theta) \tag{11}$$

where, f_c represents compressive strength of concrete; f_s represents yield stress of steel; θ represents hoop index, $\theta = A_s f_s / A_c f_c$.

2. Bearing capacity of the support

According to "technical regulation of steel tube concrete structure" (CECS 28—2012), considering the steel support in bending, under the influence of slenderness ratio and eccentricity, the ultimate bearing capacity of CFSTS is:

$$N_u = \varphi P_{\max} \tag{12}$$

where, N_u represents ultimate bearing capacity of CFSTS; $P_{\max}$ represents bearing capacity of concrete filled steel tubular stub columns under axial compression; φ represents reduction factor, considering the influence of slenderness ratio and eccentricity, $\varphi = 0.85$.

3. Calculation

Select the steel tube (Q235 steel) of Φ150 × 5 mm and the concrete of C60. The parameters of steel tube and concrete are shown in Tables 1 and 2.

The parameters in Tables 1 and 2 are substituted into the formula (9), (10), (11), (12), calculated: $P_{\max} = 2082.5$ KN, $N_u = 1770.1$ KN.

It is known that the supporting force of CFSTS is much more than that of the U-steel support by comparison. Therefore, it is very possible to use CFSTS to control the stability of surrounding rock in deep soft rock roadway. In order to improve the application of CFSTS in deep soft rock roadway, the optimization of CFSTS was studied.

Some scholars found that the axial compressive performance of CFST short columns with different cross section shape is quite different (Tu et al. 2014; Baig et al. 2006; Almadini et al. 2011). The above formula (12) demonstrates that there is the unitary relation between the axial bearing capacity of CFST short column and the ultimate bearing capacity of CFSTS. So, the mechanical properties of CFSTS with different cross section shapes are different. Thus, in order to obtain the optimal cross section shape of the steel tube, the cross section shape of the steel tube in CFSTS was studied by numerical simulation.

3 Numerical Simulation of CFSTS

3.1 Optimization of CFST Section

The cross section shape of CFST was optimized by ANSYS numerical simulation software. The deformation of steel tube was simplified as the plane strain problem with the axial strain of 0, so the force acting on the steel tube section was simplified as the force acting on the plane ring. The model is a section of circular steel tube. Using plane 42 element to simulate steel tube section, the model was set to plane-strain model and free mesh generation and divided into quadrilateral element. Fix the low end of the ring and apply loads to its upper end. When the constraints (DOF constraint) was applied, all degrees of freedom of the partial nodes in adaxial surface of the steel tube section were used as constraints. Partial nodes in abaxial surface of that was loaded with the load value of 2000 N and downward in direction. The model selects the steel tube (Q235 steel) of Φ150×5 mm and the concrete of C60. The detailed parameters of steel tube and concrete are shown in Tables 1 and 2. The model of steel tube section is shown in Fig. 4.

After calculation, the deformation of the steel tube section is shown in Fig. 5. The X, Y displacement is shown in Fig. 6 and The X, Y stress is shown in Fig. 7.

Figure 6 shows that the deformation of both sides of the steel tube in the X direction is larger, reaching to 18.6 mm; The maximum deformation and the

Table 1 The steel tube unit material parameter

Material	Poisson ratio	Elastic modulus (N/mm^2)	Plastic modulus (N/mm^2)	Yield stress (N/mm^2)	Density (g/cm^3)
Q235 Steel tube	0.280	2.06×10^5	0.15×10^5	300	7.85

Table 2 The concrete unit material parameter

Material	Poisson's ratio	Elastic modulus (N/mm^2)	Cohesion (N/mm^2)	Friction angle	Expansion angle
C60 concrete	0.2	3.65×10^4	5.5654	55.6°	30°

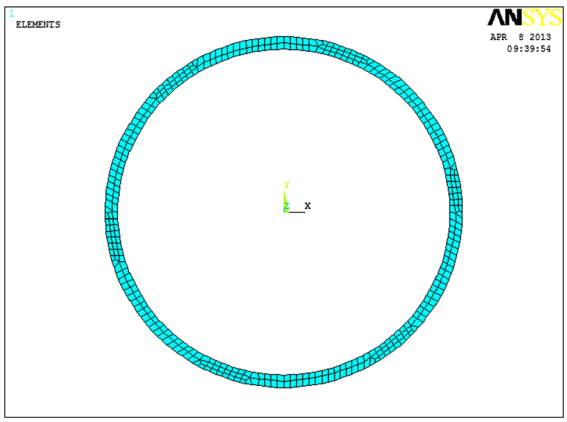

Fig. 4 The model of steel tube section

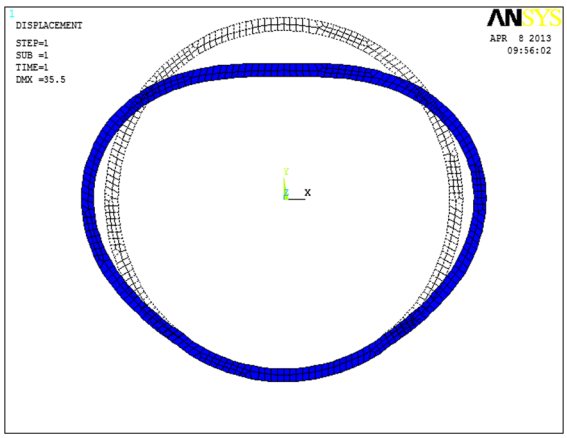

Fig. 5 The cors section of steel tube under vertical pressure

minimum deformation of steel tube are in the upper end the low end, about 35 mm and 3.8 mm, respectively.

Figure 7 shows that in the X direction, the overall stress distribution of steel tube is relatively uniform, about 1700 N. Stress concentration is appeared on the upper of the steel tube and both sides of the lower of steel tube, especially for the upper part of the steel tube that the stress is more than 12,200 N; In the Y direction, the overall stress of the steel tube is larger than that of the X direction and the stress concentration is appeared in the left shoulder of the steel tube where the stress is about 6000 N.

According to the stress and displacement analysis, the cross section shape of steel tube is closed to the capital letters D under load action. So, the D-shape is used as the cross section shape of CFST.

3.2 Axial Compression Simulation of CFST Component

The axial compression analysis of CFST short column was carried out. According to ≪Technical specification for high-rise building concrete structure≫, the axial pressure analysis of the specimens of CFST with the radial length of 140 mm and the short column length of 500 mm was carried out. Select circular CFST short column and D-shape concrete-filled steel tube (D-CFST) short column to analyze by numerical simulation. The cross section diameter of the circular steel tube is 140 mm. As the D-shape steel tube is made by the equal circumference's circular steel tube, the circumference of the D-shape steel tube is approximately equal to the circular steel tube with the diameter of 140 mm.

1. Axial compression analysis of circular CFST

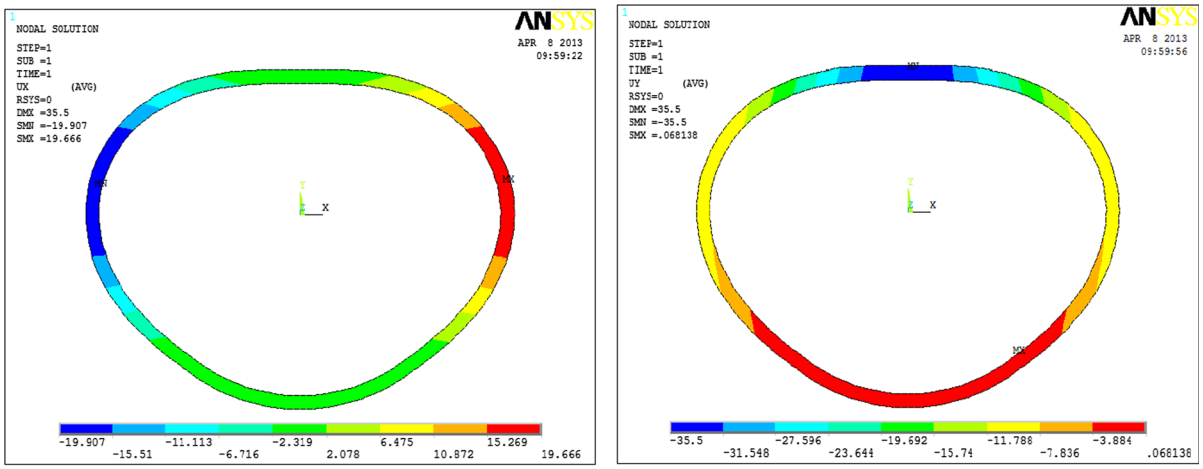

(a) (b)

Fig. 6 The displacement nephogram of X, Y

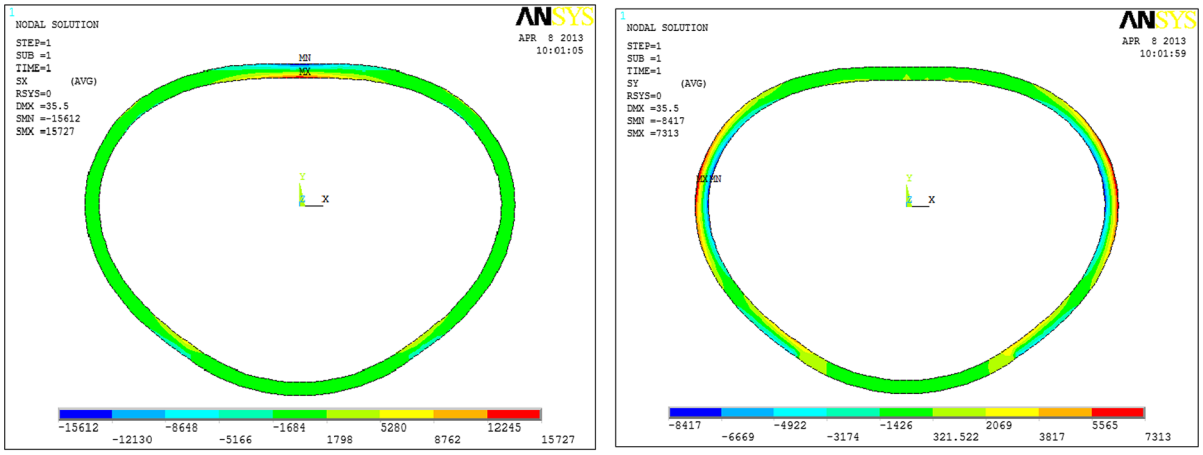

(a) (b)

Fig. 7 The stress nephogram of X, Y

The solid 45 element was used to simulate the steel tube, the solid 65 element was used to simulate the concrete, and the material was bonded with the "vglue" command. The mesh was divided into the quadrilateral element by mapping. The axial compression analysis of the circular CFST members was carried out by the way of fixing at one end and loading at the other end. The results are shown in Fig. 8.

2. Axial compression analysis of D-CFST

The short column of the D-CFST has the same deformation characteristics and material properties as that of the circular CFST. The relevant parameters of the D-CFST short column reference the short column simulation test of the circular CFST. Because of the irregular cross section of the D-shaped member, the meshing was performed by the sweep method. After meshing, one end exerted the displacement constraint and the other side exerted the surface load in the model. The results are shown in Fig. 9.

3. Simulation result analysis

Based on the axial compression analysis of the circular and D-shape CFST in Figs. 8 and 9, the conclusions are drawn: In the same length and

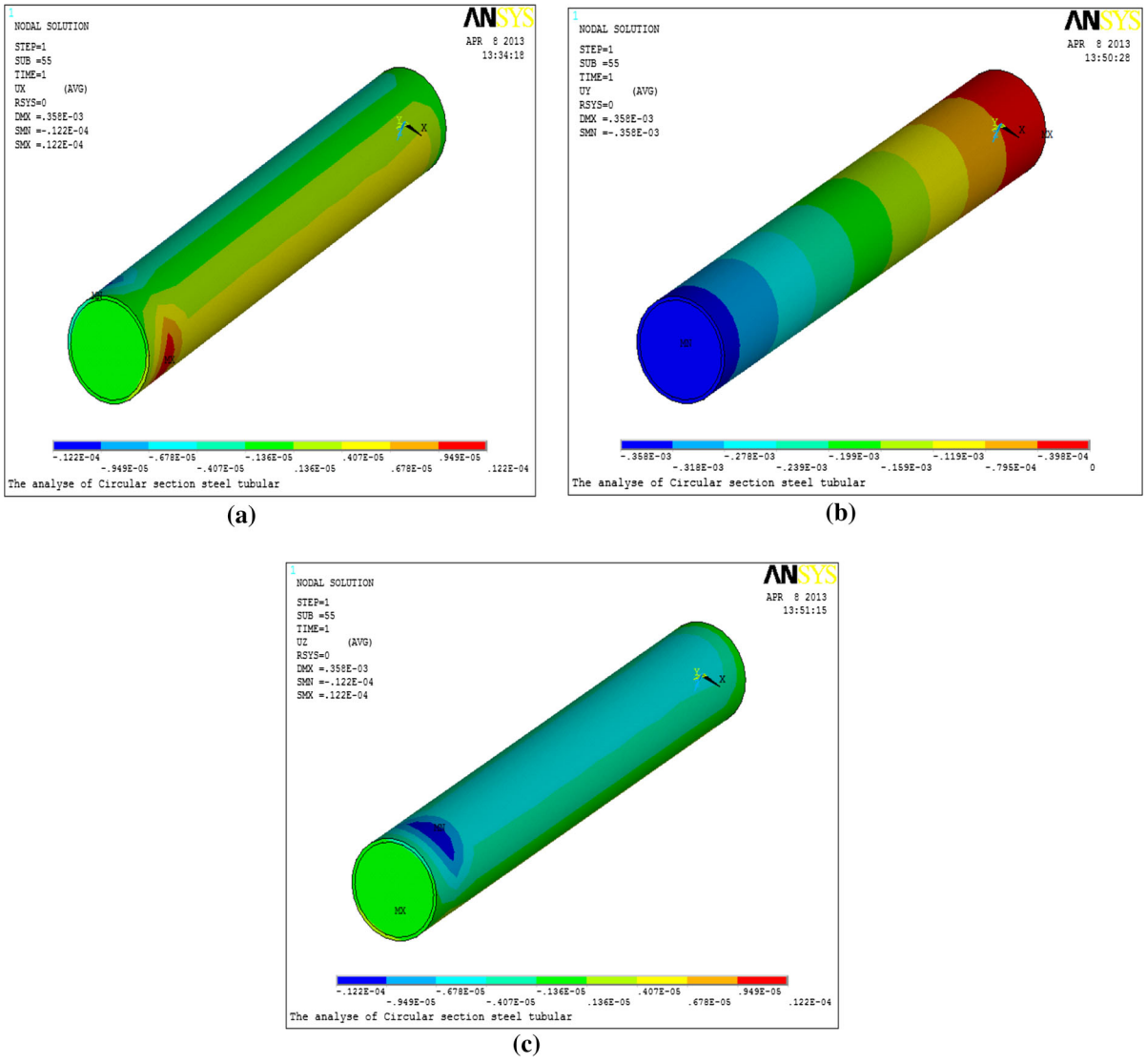

Fig. 8 The displacement nephogram of X, Y, Z

circumference of steel tube, the displacement of the circular CFST is 0.19 mm and the displacement of D-CFST is 0.148 mm by applying the same size load. According to the comparison of displacement, the compressive strength of D-CFST is larger than that of circular CFST. In the following analysis, the bending strength of the D-CFSTS and the circular CFSTS was calculated by numerical simulation. It is further confirmed whether the D-CFSTS can meet the requirement in deep mine roadway.

3.3 Mechanical Analysis of CFSTS

1. Scheme design and model optimization

According to the above analysis, it is confirmed that the bending strength of the D-CFSTS is much large than that of the circular CFSTS. Now, the shape of the CFSTS structure is designed to be horseshoe-shaped. Then the overall performance of the D-CFSTS and the circular CFSTS is compared and analyzed whether the D-CFSTS has advantages in structure.

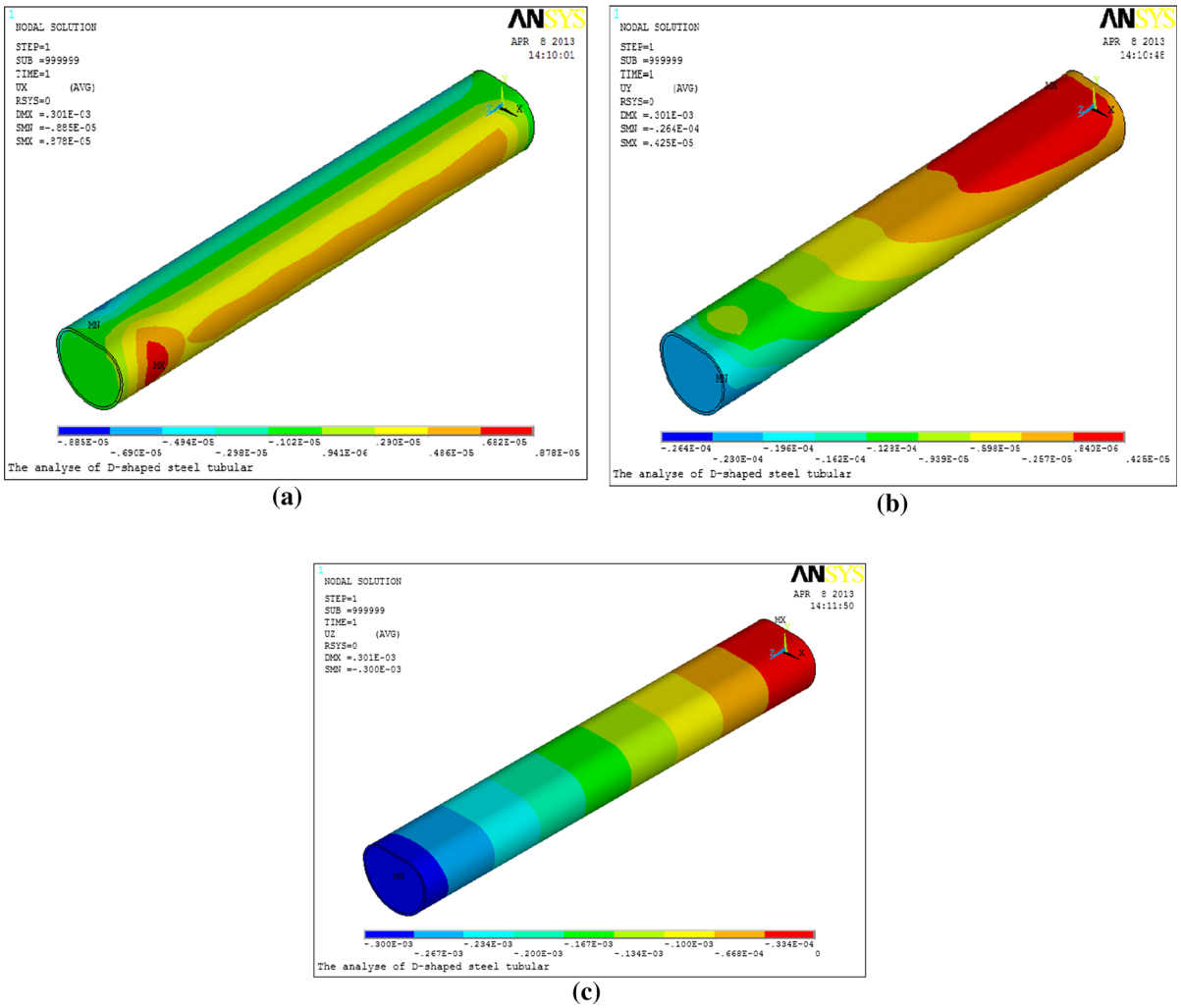

Fig. 9 The displacement nephogram of X, Y, Z

The boundary conditions of designing support: The bottom of support is fixed and the top arch of that is subjected to stress analysis; Taking into account the impact of horizontal stress on the support, applying pressure to the side arch is the same as that in the top arch. According to the geological conditions, the pressure is estimated to be 15MP. So, add the surface force of 15MP to the top arch and side arch of the support at the same time. In order to facilitate the calculation, the horseshoe-shaped support was simplified as the semi-circular arch supports. The simplified model is shown in Fig. 10. This model is mainly composed of the top arch section and two side arch sections of the horseshoe-shaped support that three arch sections are the same and the corresponding

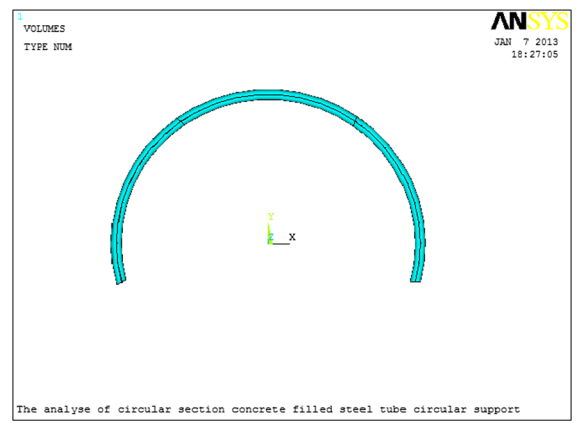

Fig. 10 Simplified model of CFSTS

center angle of each arch section is 70°. Then, the same load was applied to the top arch section and two side arch sections of the model, at the same time, the displacement constraints are applied to the two end of arch support.

2. Compression analysis of CFSTS

After calculation, the displacement of the D-CFSTS is shown in Fig. 11:

After calculation, the displacement of the circular CFSTS is shown in Fig. 12:

The displacement diagram shows: when the uniform load was applied to the specimens, the deformation at the top of the specimens is the largest. Due to the bottom of support is fixed, the deformation is close to 0 and the deformation from the bottom to the top is gradually increased. It shows that the simulated result are in accordance with the theory and the experimental data is of reference value.

As can be seen from Figs. 11 and 12, the displacements of the D-CFSTS and the circular CFSTS are 0.004596 and 0.94863 mm, respectively. It shows that when the same load is applied to the CFSTS, the deformation of the circular CFSTS is much larger than that of the D-CFSTS. The bending strength of the D-CFSTS is higher than that of the circular CFSTS.

3.4 Stress Analysis of the Support Under Different Stress Conditions

The horizontal stress is often higher than the vertical stress in deep mine. So, this paper studied the mechanical properties of the support under different side pressure coefficient. The mechanical properties of

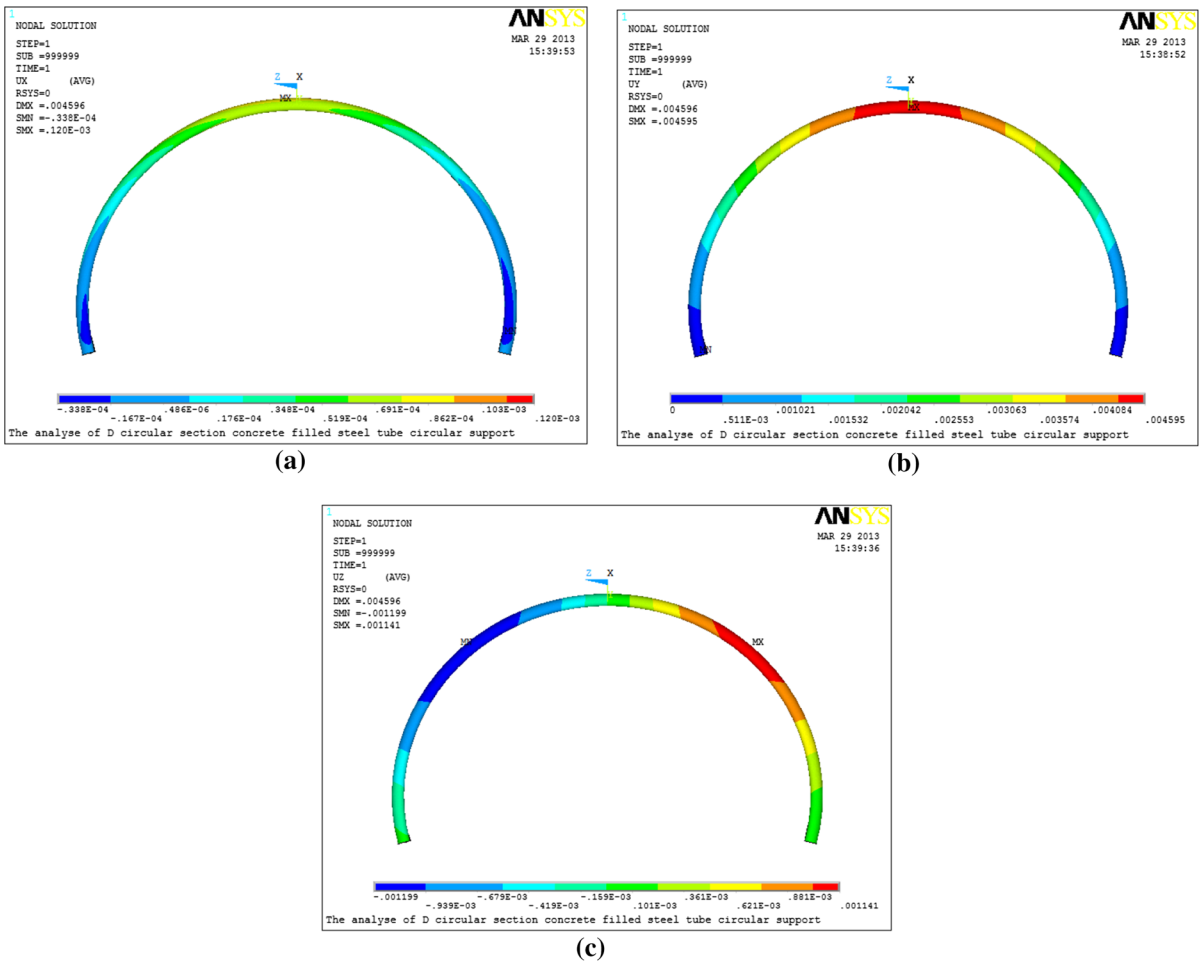

Fig. 11 The displacement diagram of X, Y, Z of the D-CFSTS

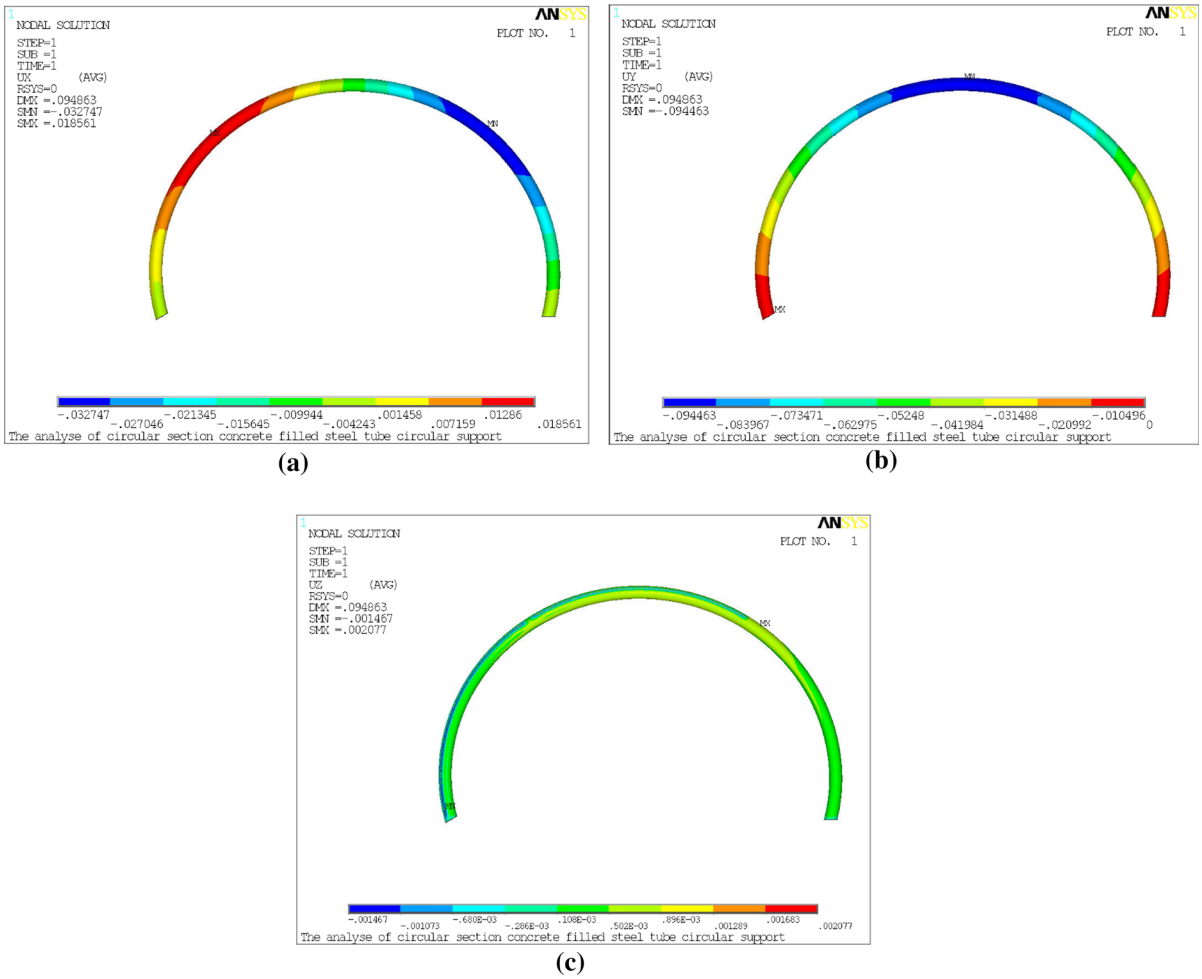

Fig. 12 The displacement diagram of X, Y, Z of the circular CFSTS

the circular CFSTS and the D-CFSTS was mainly studied when the ratios of the horizontal stress and the vertical stress are 1.5 and 2. Apply the same stress to the two kinds of supports and analyze the deformation of the supports.

In order to make loading easier, the circular CFSTS and the D-CFSTS were changed into three equal sections of the support. Apply the different load to the three sections of the support, respectively. The model after loading is shown in Fig. 13:

1. Stress analysis of the support when the ratio of horizontal stress and vertical stress is 1.5

Figure 14 is the displacement diagram of the circular CFSTS. Figure 15 is the displacement diagram of the D-CFSTS. Figures 14 and 15 show that the displacement of the D-CFSTS is 0.71 and

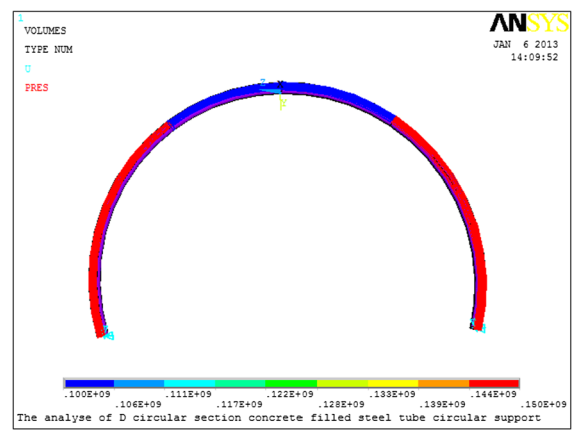

Fig. 13 The model after loading

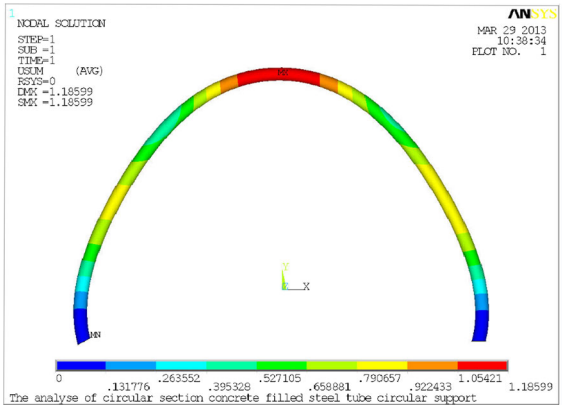

Fig. 14 The displacement diagram of the circle CFSTS

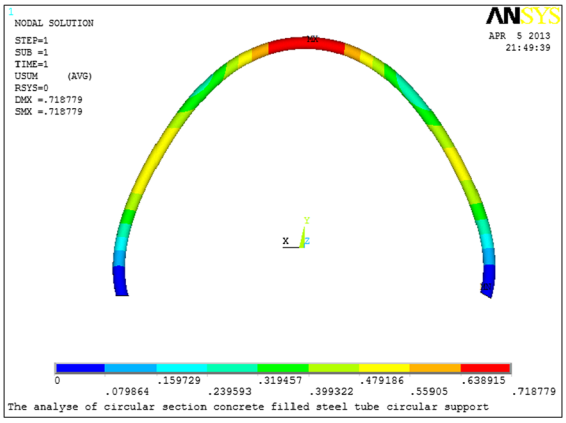

Fig. 15 The displacement diagram of the D-CFSTS

the displacement of the circular CFSTS is 1.19. The displacement of the D-CFSTS is much smaller than that of the circle CFSTS. It can be concluded that: In the case of the ratio of horizontal stress and vertical stress of 1:1.5, the mechanical properties of the D-CFSTS is better than the circular CFSTS.

2. Stress analysis of the support when the ratio of horizontal stress and vertical stress is 2

Figure 16 is the displacement diagram of the circular CFSTS. Figure 17 is the displacement diagram of the D-CFSTS. Figures 16 and 17 show that the displacement of the D-CFSTS is 1.49 and the displacement of circular CFSTS is 2.46. The deformation of the D-CFSTS is much smaller than that of the circle CFSTS. It can be concluded that: in the case of the ratio of horizontal stress and vertical stress of

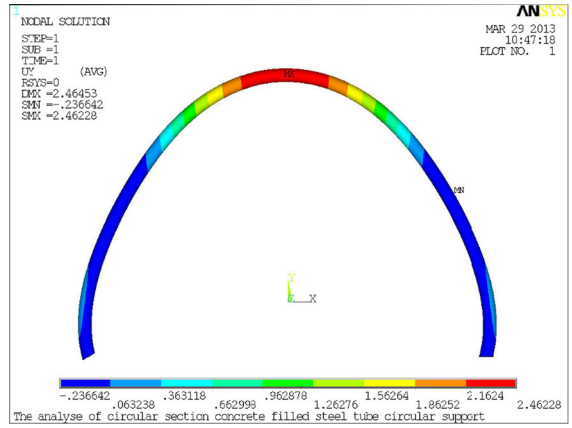

Fig. 16 The displacement diagram of the circle CFSTS

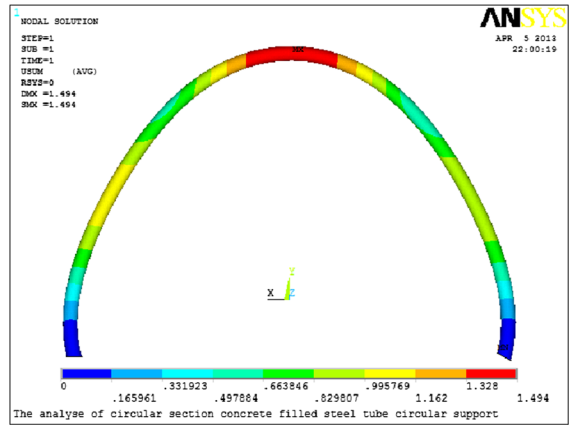

Fig. 17 The displacement diagram of the D-CFSTS

1:2, the stress state of the D-CFSTS is better than the circular CFSTS.

3. Summary of support force analysis

When the ratios of the horizontal stress and the vertical stress are 1:1.5 and 1:2 in deep mine, the deformation of the D-CFSTS is much smaller than that of the circle CFSTS under the same load. It can be concluded: when the horizontal stress is greater than the vertical stress, the stress state of the D-CFSTS is better than that of the circular CFSTS, the D-CFSTS is more suitable for deep tunnel support than the circular CFSTS.

4 Making Process

Adopt the concrete mixing technology by Sand Envelope with Cement. Construction procedure: Firstly, put the sand and the water and agitate; Secondly, put the cement and agitate; Thirdly, put the carpolite and agitate; Lastly, put the water and admixture and agitate. The manufacture of CFSTS is completed in three steps: tube bending, support assembly, concrete casting.

1. Steel tube bending. The cold pressing method is adopted to bend the steel tube. The cross section of steel tube is processed into D-shape by round and the steel tube is bent a certain radian by the cold pressing method. The steel tube surface is smooth without damage or fold.
2. Support assembling. Each section of CFST is connected by the casing. The support is assembled on the ground and the assembled support are marked. After labeling, assemble the support in the mine according to the sequence number. Before assembling, the end of the steel tube is polished to ensure the uniform force on the sections of the CFSTS.
3. Concrete placing. Pour concrete from the top of the steel tube by the special pumpcrete machine. After pouring 1/3 height, vibrate the CFSTS every 1/3 height. In order to compensate for the loss caused by the solidification of the concrete at the top of the grouting hole, after 24 h, the supplementary pouring for the CFSTS that has been poured is carried out, until the grouting hole is opened.

5 Engineering Application

5.1 Engineering Situation

Pingdingshan ten mines is located in the hilly country of the Ruhe south and the Shahe north. The terrain of mine field in the northwest is higher than that in the southeast. The strike length of the mine field from the east to west is 5.6 km and the inclination length of that from the north to the south is 7.0 km. The gross thickness of coal measures is about 900 m. The gross thickness of the main mineable coal is 13.74 m. The inclination angle of coal seam is 0–35°. Because of the occurrence condition of coal seam and the mountain in ground surface, the buried depth of coal seam is about 450–1100 m. The immediate roof and the immediate floor of coal seam are mainly sandy mudstone and mudstone and the basic roof and the basic bottom of that are mainly sandstone.

Mine had been using U-steel support to support roadway. Due to the influence of mining-induced stress and weak broken wall rock, the floor heave, rib spalling and slurry cracking in—320 level ventilation roadway of Pingdingshan ten mines were serious and the roadway needs to be repaired once or twice a year. In order to seek a more economical, safe and reliable support way than the original support way and verify the reliability of the newly designed D-CFSTS, the D-CFSTS and the U-steel support were adopted respectively in the two sections of 100 m test roadway of Pingdingshan ten mines. Then the supporting effect was compared and analyzed.

5.2 Design of Roadway Support

In one section of the test roadway, the above mentioned D-CFSTS was adopted as the main support way. The design structure and the actual supporting effect are shown in Figs. 18 and 19, respectively. In the other section of the test roadway, the U36 steel support was used to support the roadway, and the design structure is shown in Fig. 20.

The components parameters of the D-CFSTS: Select the steel tube (Q235 steel) of Φ150 × 5 mm

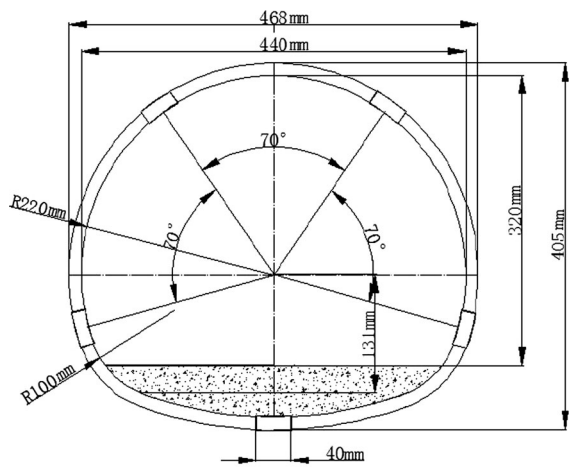

Fig. 18 Structure figure of curved D-CFSTS

Fig. 19 Actual supporting effect figure of curved D-CFSTS

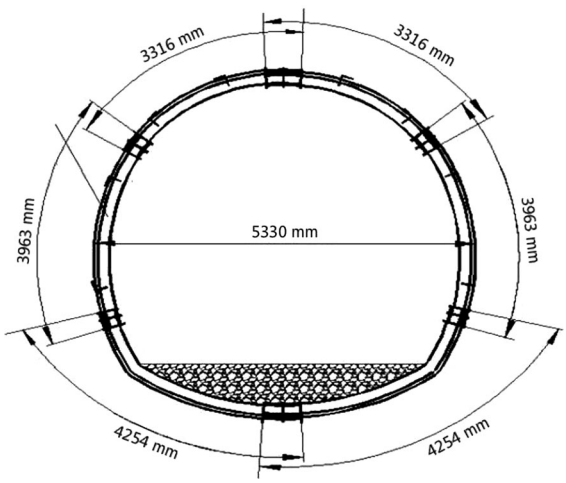

Fig. 20 Structure figure of U-steel support

and the micro expansion concrete of C60. The circumference, width, height and spacing of the support are 11530, 4680, 4050 and (650 + 50) mm, respectively. The size of the casing is Φ165 × 6.5 mm and the length of that is 400 mm. The support is horseshoe shaped and is divided into four sections.

The components parameters of U-steel support: The circumference, spacing, width and height of U36 steel support are 12350, (650 + 50), 4530 and 3980 mm. The support is arched and is divided into six sections. The sections were connected by cable connection. Each lap joint must be connected with three clips that the lap length is 400 mm.

5.3 Observation of Supporting Effect

There are the total of 153 supports in the two sections of the test roadway. One observation point was set for every 6 supports. A total of 25 observation points numbered as 1#–25# points, respectively.

Mine pressure observation is an effective means to test the effect of roadway support, mainly by observing the deformation of roadway surrounding rock. In order to confirm the rationality of the support way, the observational data mainly include the displacement of the roadway's sides and the top-floor. The observation time was from August 2015 to March 2016.

After a period of time, the roadway of U-steel support test section could not meet the requirements of mine production and use because of support damaging and oversize roadway deformation. So, the observational data of of U-steel support test section was of no analytical significance. The surrounding rock of the roadway in test section of D-CFSTS was stable after small deformation and the roadway could be used for a long time. In this paper, select the representative points of the roadway in test section of D-CFSTS for analysis. The displacement evolution law of the top-floor and the roadway's sides in the measuring point are shown in Figs. 21, 22 and 23.

Because there was a certain gap between the D-CFSTS and the roadway wall, the support was not fully played in the early stage. So, the roadway roof subsidence was obvious and the change rate was fast. After a period of time, the roadway surrounding rock and the D-CFSTS started the real contact and the obvious supporting effect began to appear. With the gradual expansion of the contact area, the supporting effect of the D-CFSTS increased gradually and the displacement rate of the roadway was reduced significantly. Finally, the relative displacement of the roadway was unchanged essentially. Due to the overall effect of the support, the roof subsidence of the roadway had led to the outward expansion of the roadway's sides and the roadway's sides showed a gradual evolution trend. In the whole observation process, the D-CFSTS was in good condition and had no obvious damage.

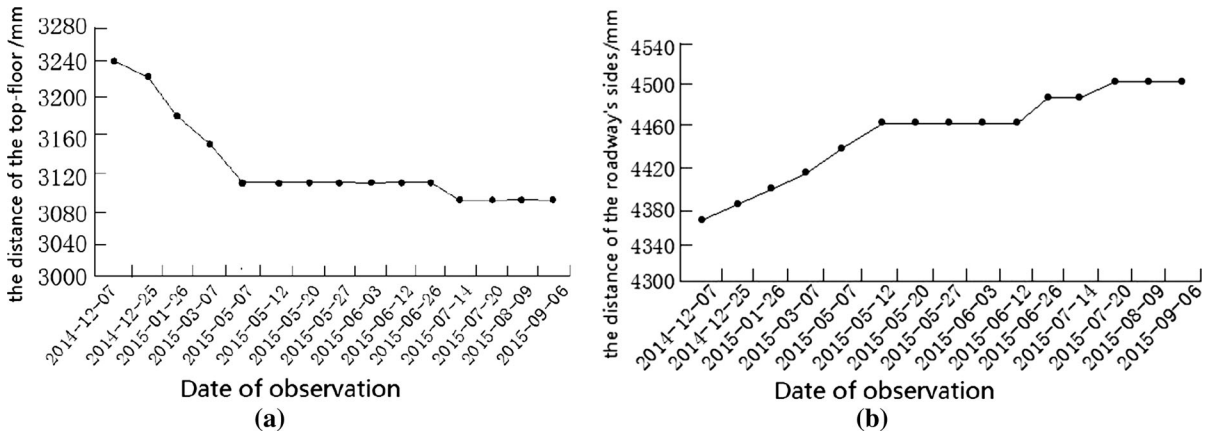

Fig. 21 The displacement evolution law of roadway in the measuring point 3. **a** The top-floor distance, **b** the roadway's sides distance

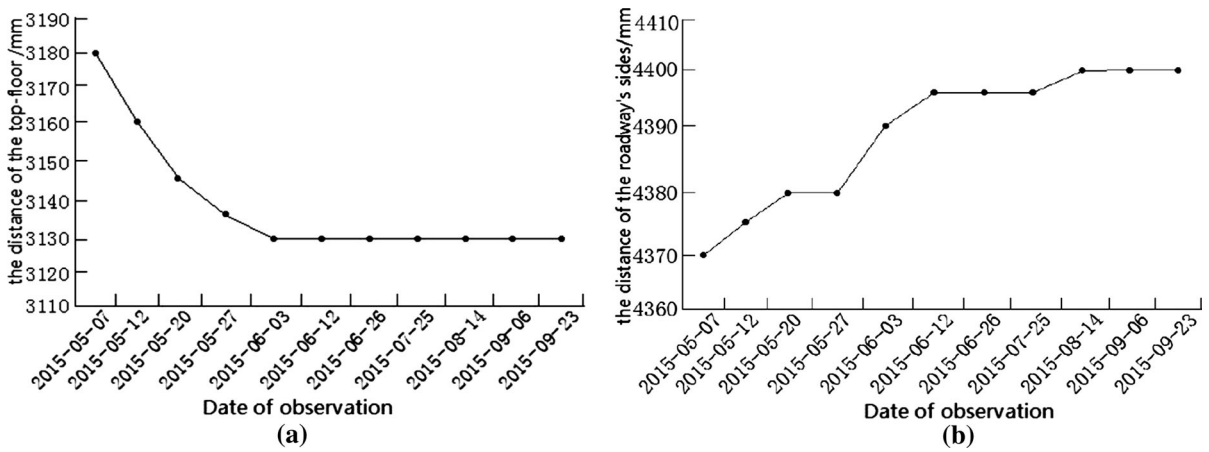

Fig. 22 The displacement evolution law of roadway in the measuring point 13. **a** The top-floor distance, **b** the roadway's sides distance

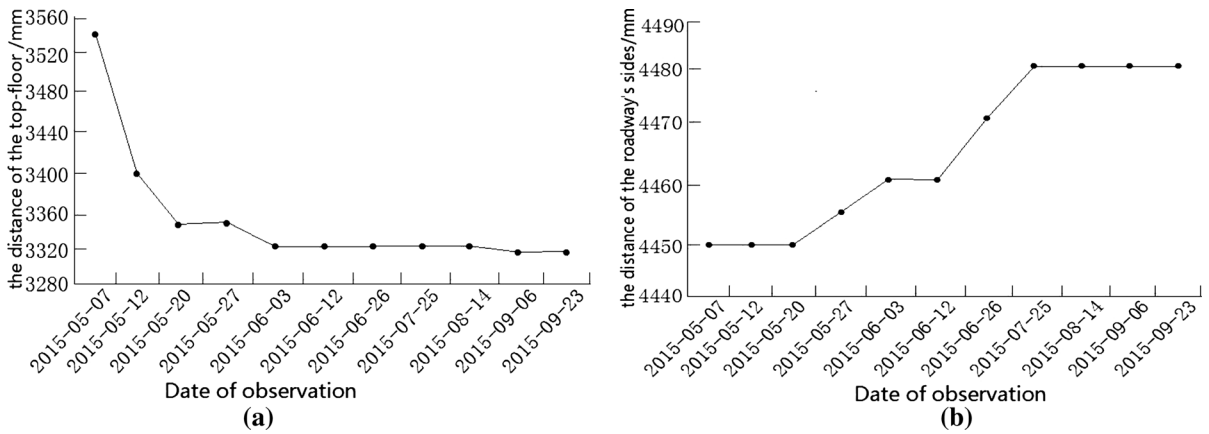

Fig. 23 The displacement evolution law of roadway in the measuring point 17. **a** The top-floor distance, **b** the roadway's sides distance

Table 3 The parameter of the two supporting ways

Supporting materials	Section size (mm)	The area of steel in the section(mm^2)	Unit mass (g/mm)
U-steel support (U36)	U36	4570	35.87
D-CFSTS	Φ150×5 mm	2355	18.48

5.4 Evaluation of Economic Benefit

1. Supporting costs of two supporting ways

Mainly used the D-CFSTS (made by the circular steel tube) and U-steel support respectively in the two sections of the test roadway. The parameter of the two supporting ways are compared, as shown in Table 3.

① Supporting costs of the D-CFSTS (the support circumference was calculated by 12000 mm): 1231 yuan.
② Supporting costs of U-steel support (the support circumference was calculated by 12000 mm): 2165 yuan.

Compared with the U-steel support, the single D-CFSTS had saved the cost of 934 yuan and reduced the use of about 208 kg of steel and the cost of about 43% of the cost of single support material.

2. Comparison of support efficiency

① Cost–benefit of new supporting section

In the 100 m long roadway, the row distance is 650 mm, so a total of 153 supports are required. According to the above calculation, the roadway support cost of the D-CFSTS is 142902 yuan less than that of the U-steel support.

② Rework benefit of new support section

The roadway of the U-steel support is repaired at least once a year. The cost of repairing each meter is about 3000 yuan. However, the roadway of the D-CFSTS has been nearly a year without repairation. So, the repairable cost of the test section of 100 m saved 300,000 yuan.

Synthesis (1), (2), the use of D-CFSTS for each 100 meters of roadway could save 442.9 thousand yuan than that of U-steel support.

③ Promotion benefit

The annual excavation length of similar roadway in Pingdingshan ten mine is about 3000 meters. If 2000 meters can use the D-CFSTS, the cost of support could save $(142{,}902 + 300{,}000) \times 20 = 8{,}858{,}040$ yuan (that is 8858.04 thousand) and about 636 tons of steel.

6 Conclusion

Due to the traditional support way can not meet the needs of the support in the high stress soft rock roadway, this paper improved and expanded the application of the CFSTS in deep roadway support. Then a systematic study was carried out through the theoretical calculation, numerical simulation and engineering application. The following conclusions may be drawn:

1. The supporting force of the CFSTS and the U-steel support were calculated by theoretical calculation. The supporting force of U-steel support is smaller than that of the CFSTS. With the increase of the ratio of the horizontal stress and the vertical stress, the supporting force of the support is gradually reduced.
2. By numerical simulation software, the shape of the steel tube section was optimized and designed as the D-shape. The compressive strength of the D-CFST is larger than that of the circular member. When the same load is applied to the CFSTS, the deformation of the D-CFSTS is far less than that of the the circular CFSTS. When the horizontal stress is greater than the vertical stress, the stress state of the D-CFSTS is better than that of the circle CFSTS. So, the D-CFSTS is more suitable for the deep roadway support.
3. The roadway of U-steel support test section could not meet the requirements of mine production and use because of support damaging and oversize roadway deformation. In the whole observation process, the D-CFSTS was in good condition and

the deformation of the surrounding rock was not large. By calculation, the cost of roadway per 2000 meters could be saved $(142{,}902 + 300{,}000) \times 20 = 8{,}858{,}040$ yuan (that is 8858.04 thousand) and about 636 tons of steel.

Acknowledgements The work described in this paper was fully supported by Student Science and Technology Innovation Fund Foundation of College of Mining and Safety Engineering in Shandong University of Science and Technology (KYKC17009).

References

Aghdamy S, Thambiratnam DP, Dhanasekar M et al (2015) Computer analysis of impact behavior of concrete filled steel tube columns. Adv Eng Softw 89:52–63

Almadini M, Kovacevic D, Radonjanin V (2011) Comparative analysis of axially loaded composite columns. Appl Mech Mater 147:99–104

Baig MN, Fan JS, Nie JG (2006) Strength of concrete filled steel tubular columns. Tsinghua Sci Technol 11(6):657–666

Dong CX, Kwan AKH, Ho JCM (2017) Effects of external confinement on structural performance of concrete-filled steel tubes. J Constr Steel Res 132:72–82

Gao YF, Wang B, Qu GL et al (2009) Mechanical performance test of concrete filled steel tubular support and its application in roadway support. The eighth cross strait tunnel and underground engineering academic and technical seminar, China Taibei 11: C15-1-C15-10. (**in Chinese**)

Gao YF, Wang B, Wang J et al (2010) Test on structural property and application of concrete-filled steel tube support of deep mine and soft rock roadway. Chin J Rock Mechan Eng 29(1):2604–2609 **(in Chinese)**

Gu LX, Ding FX, Fu L et al (2014) Mechanical behavior of concrete-filled round-ended steel tubular stub columns under axial load. China J Highw Transp 27(1):57–63

Guo L, Li R, Fan F et al (2012) Study on hysteretic behaviors of composite frame-steel plate shear wall structures. China Civil Eng J 45(11):69–78

Han LH, Liao FY, Tao Z et al (2009) Performance of concrete filled steel tube reinforced concrete columns subjected to cyclic bending. J Constr Steel Res 65(8–9):1607–1616

Liu L, Zhang J (2017) Thermal insulation composite material for Governance of underground thermal hazard and its application. J Shandong Univ Sci Technol (Natural Science Edition) 36(1):46–53

Meng QB, Han LJ, Qiao WG et al (2012) Mechanism of rock deformation and failure and monitoring analysis in water-rich soft rock roadway of western China. J Coal Sci Eng (China) 18(3):262–270

Nie JG, Wang YH, Fan JS (2014) Study on seismic behavior of concrete filled steel tube columns under pure torsion and compression-torsion combined action. China Civil Eng J 47(1):47–58

Thayalan P, Aly T, Patnaikuni I (2009) Behaviour of concrete-filled steel tubes under static and variable repeated loading. J Constr Steel Res 65(4):900–908

Tu YQ, Shen YF, Li P (2014) Behaviour of multi-cell composite T-shaped concrete-filled steel tubular columns under axial compression. Thin-Walled Struct 85:57–70

Wang B (2009) Analysis on the laws of tunnel deformation in soft rock and the supporting technology of concrete-filled steel tube support. China University of Mining and Technology (Beijing), Beijing. (**in Chinese**)

Xu C, Luo XL, Zhu CX et al (2014) Analysis of circular concrete-filled steel tube (CFT) support in high ground stress conditions. Tunn Undergr Sp Technol 43:41–48

Yang SQ, Chen M, Jing HW et al (2017) A case study on large deformation failure mechanism of deep soft rock roadway in Xin'An coal mine, China. J Eng Geol 217:89–101

Zhou JF (2010) Research of application of controlling deformation by yield-rigid U section steel support in the soft rock main road of Ningzhuang coal mine. Henan Polytechnic University. (**in Chinese**)